

Available online at [www.sciencedirect.com](http://www.sciencedirect.com)**ScienceDirect**

Procedia Materials Science 5 (2014) 598 – 604

**Procedia**  
Materials Science[www.elsevier.com/locate/procedia](http://www.elsevier.com/locate/procedia)International Conference on Advances in Manufacturing and Materials Engineering,  
AMME 2014

## Evaluation of contact stresses in bearings made of Al – Beryl Metal Matrix Composites by Finite Element Method.

V. Bharat<sup>a,b</sup>, B. Durga Prasad<sup>b</sup>, N.J. Krishnaprasad<sup>c</sup>, K. Venkateswarlu<sup>d\*</sup><sup>a</sup>HKBK College of Engineering, Bangalore, 560045, India<sup>b</sup>Department of Mechanical Engineering, JNTU, Anantapur, 515002, India<sup>c</sup>Bangalore Institute of Technology, Bangalore, 560004, India<sup>d</sup>CSIR-National Aerospace Laboratories, Bangalore, 560017, India

### Abstract

In the present investigation, interference fitted assemblies were analyzed using finite element method to evaluate contact stresses. The main objective of this research work is to develop metal matrix composite of commercially available pure aluminum reinforced with different weight percentage of Beryl to attain a most desirable property combination for bearings. A detailed analysis on the effect of bearing material on contact stresses was undertaken. The work covers the analysis based on Hertzian contact stresses. An appropriate finite element model was developed to analyze the pattern of contact stresses in the interference assemblies. Ansys workbench was used as a tool to construct the model and to perform analysis. The model was simulated by applying a pressure of 100 MPa and at different speeds of the shaft. A comparative study on the effect of bearing materials such as bronze, Al-SiC and Al-Beryl MMCs on contact stresses were clearly demonstrated. It has been found that the contact stresses in the bearings made of Al-Beryl metal matrix composite was in the range of 4678.7 to 4680 Pa at different speeds which was very much less when compared to the bronze and Al- SiC MMC. The results clearly demonstrated Al-Beryl can be used as one of the most suitable materials for fabricating bushes.

© 2014 Elsevier Ltd. This is an open access article under the CC BY-NC-ND license (<http://creativecommons.org/licenses/by-nc-nd/3.0/>).

Selection and peer-review under responsibility of Organizing Committee of AMME 2014

*Keywords:* Aluminum; Beryl; Contact stress; Bushes; Finite element analysis

\* Corresponding author. Tel.: 080 - 25086244; fax: 080 - 25270098.  
E-mail address: [kvenkat@nal.res.in](mailto:kvenkat@nal.res.in)

## 1. Introduction

A strong demand for weight reduction urges the optimization of the design of products employing light weight materials. The replacement of conventional materials by lighter metals such as aluminum is, therefore, highly desirable. However, Aluminium alloys are not sufficiently stiff or strong for many purposes and their reinforcement is necessary [M.K. Surappa et al. (2011)]. Aluminium based MMCs are widely used for these applications owing to the high ductility of the matrix and the high strength of the hard reinforcing phases. AMCs have very high specific modulus, strength to weight ratio, fatigue strength and wear resistance. [D. D. L. Chung et al. (2003)]. The presence of reinforcing particles produces potential properties non-attainable by other materials. AMCs have emerged as the important class of advanced materials giving engineers the opportunity to tailor the material properties according to their needs. Essentially these materials differ from the conventional engineering materials from the viewpoint of homogeneity. [H. Akbulut et al. (1998)]

Among various ceramic additions to Al, SiC has been given greater attention by many researchers. However, Al-SiC MMC still has some limitations such as the formation of  $Al_4C_3$  during high temperature synthesis, which impairs poor mechanical properties. Thus, efforts have been made to overcome the problems by incorporating other reinforcing materials such as Beryl [N.J. Krishna Prasad et al, (2012)]. The density of beryl is almost equivalent to Al and fairly lower than SiC, in the present investigation, it is aimed to reinforce beryl in Al matrix. Beryl, which is naturally occurring and having the formula  $(Be_3Al_2Si_6O_{18})$  was used as the reinforcing agent, while commercially available pure aluminum has been used as the matrix. The beryl particles used were of 30 and 106  $\mu m$  size. They exhibited density value of 2.6-2.8  $g/mm^3$ , hardness of 7.5 to 8.5 on Mohs scale and of hexagonal structure [H.B. Bhaskar et al. (2012)]. When processed through powder metallurgy route, Al-Beryl MMCs exhibit excellent tribological properties and can be competent material for manufacturing bearings and bushes.

In many applications, it is important to study the stresses that arise at contact regions of interference fitted assemblies. Such applications include bearing bushes, pump impeller on shaft, small end bush in connecting rod, a crank pin in a cast iron web, liners in cylinder blocks, valve seats, gears, locomotive wheel on axle, stator of a fan, fitting rotors on turbines and compressors on shafts and mechanical drives and assembling of bearing races [Irappa Sogalad et al. (2006)]. Contact stresses leads to high stress concentration and can lead to plastic deformation which leads to reduction in load bearing capacity of a structure. Mechanics of the shaft and bush contact is one of the elemental and basic areas of the study in mechanical engineering, requiring both very important and large application skill and reliable analysis approaches. Analytical formulations depicting the physics of this fact are defined only for special type of simple contact geometries, so for more intricate and complex geometries the analytical models employing closed forms remain hard to comprehend [Vahid Monfared, (2012)]. Finite element analysis (FEA) can be successfully applied as one of the numerical computation methods into bush–shaft contact problems to verify their results by comparing them to their actual life information determined over the past years.

In this work an attempt has been made to study contact stresses between shaft and bush made of Bronze, Al-SiC and Al-Beryl and critical geometric features like length of contact, mating diameter and amount of interference on stress distribution at the interface of the shaft and the bush of the interference fitted assembly [Irappa Sogalad et al. (2006)].

## 2. Materials and Process

In the present study, commercially pure aluminium powder of 99.7 % purity selected as the base material. The chemical composition of Al powder is as shown in table 1. Beryl was used as reinforcement particles. The percentage of Beryl was varied from 5 to 15 % steps of 5 wt. %. Chemical composition of beryl by weigh percentage is as shown in table 2 [Reddappa H.N et al. (2011)]. The particle size was varied from  $30 \pm 5 \mu m$  and  $106 \pm 5 \mu m$ . Powder metallurgy was used to prepare the composite specimens and is one of the most common routes to synthesize a metal-matrix composite. In this process, the required amounts Al and Beryl powders were taken in separate batches. The powder mixture was thoroughly mixed using agate motor, and cylindrical pellets of diameter 26 mm were prepared by applying a pressure of 200 MPa. These compacted pellets were sintered using Microwave sintering at a temperature of 500 to 600 °C [K. Venkateswarlu et al, (2010)]. The sintered samples were polished and prepared for hardness determination and metallographic examination. Various components can be formed with the

powder compaction process. Some examples of these parts are bearings, bushings, gears, pistons, levers, and brackets. When pressing these shapes, very good dimensional and weight control are maintained. In a number of these applications the parts may require very little additional work for their intended use; making for very cost efficient manufacturing.

Table 1(a) Chemical composition of Pure Al by weight percentage

| Element | Si   | Fe   | Al      |
|---------|------|------|---------|
| Wt. %   | 0.14 | 0.16 | Balance |

Table 1(b) Chemical composition of beryl by weight percentage

| Element | SiO <sub>2</sub> | Al <sub>2</sub> O <sub>3</sub> | BeO  | Fe <sub>2</sub> O <sub>3</sub> | CaO  | MgO  | Na <sub>2</sub> O | K <sub>2</sub> O | MnO  |
|---------|------------------|--------------------------------|------|--------------------------------|------|------|-------------------|------------------|------|
| Wt. %   | 65.4             | 17.9                           | 12.3 | 0.8                            | 1.34 | 0.48 | 0.55              | 0.004            | 0.05 |

### 3. Experimental methods

Contact problem is highly nonlinear and requires significant computer resources to solve, and it presents two significant difficulties. First, the regions of contact are unknown. Contact surfaces can come into and go out of contact with each other in a largely unpredictable and abrupt manner. Second, most contact problems need to account for friction.

The response of the bearings under loading was investigated using the finite element model. A prototype model of shaft and bush were used to simulate the analysis. Shaft was made to rotate at different speeds and the contact stress and deformation were evaluated. The size of the shaft and the bush are selected according to many practical applications and details are given in Fig. 1. For the analysis, different combinations of shaft and bush made of Bronze, Al-SiC and Al – Beryl composites are considered. The composite materials are considered in the present study are based on i) mechanical properties such as high resistance to wear and corrosion and strength, ii) commonly used bearing materials, iii) stress withstanding capacity, iv) weight of the material and, v) cost and availability of the material [M. Dhana balakrishnan et al. (2013)].

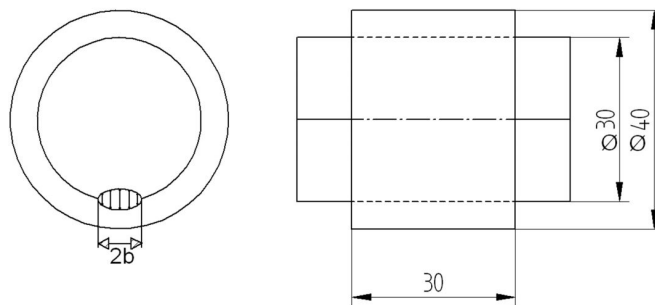


Fig 1: Shaft and bush assembly with contact zone.

Hertz's contact stresses are used to determine the contact stress at the interference. The half width 'b' of the contact area of shaft and bush is given by

$$b = \sqrt{\frac{4F \left[ \frac{1-\nu_1^2}{E_1} + \frac{1-\nu_2^2}{E_2} \right]}{\pi L \left( \frac{1}{R_1} + \frac{1}{R_2} \right)}} \quad (1)$$

Where E1 and E2 are the moduli of elasticity for the shaft and the bush and  $\nu_1$  and  $\nu_2$  are the Poisson's ratios and L is the length of contact. The contact pressure along the centre line of contact area is given by:

$$P_{\max} = \frac{2F}{\pi b L} \quad (2)$$

The maximum principal stress generated at the contact zone is given by

$$\sigma_1 = 2\nu P_{\max} \left[ \sqrt{\frac{z^2}{b^2} + 1} - \left| \frac{z}{b} \right| \right] \quad (3)$$

Finite element analysis has been used to investigate the stresses produced at the surface of the joint. The model considered for the analysis is symmetric in respect to geometry and loading [L.A. Dobrzański et al, (2009)]. A 3D model was analysed using ANSYS workbench. Stress distribution at the contact surface was the main concern.

This 3D model was prepared in Ansys workbench and geometry is transferred to the ANSYS software. The following contact options are set for all analyses. Contact face: inner face, Conta172 element, Unsymmetrical contact, Friction coefficient =0.2, default options otherwise specified. The meshed model is as shown in Fig. 2. To take the benefit of the symmetry of the problem, quarter portion of the model was considered for the analysis. Finite element model mesh is obtained having a total of 107040 elements and 461052 nodes.

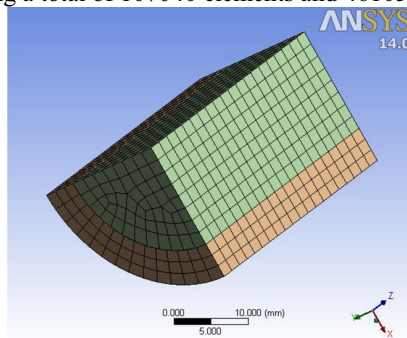


Fig 2: Shaft and bush assembly with contact zone.

A pressure equal to 100 MPa is induced at the position of contact of shaft and the bush. Shaft made of medium carbon steel is made to rotate by varying speeds and the model is tested by varying materials of the bush. Figure 3 shows the boundary conditions of the model to analyze using FEM.

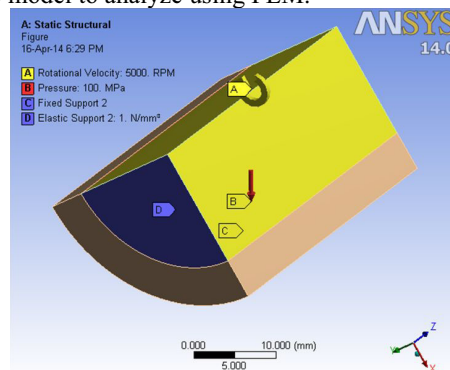


Fig 3: Boundary conditions in Finite Element Model.

### 4. Results and Discussion

In this section, results of the numerical analysis by finite element method (FEM) in shaft – bush assembly are presented. Stress and deflection analysis were carried out using finite element method. Equivalent stress in bush and shaft has been analysed by FEA and statistically shown as Fig 4. Figure 4 shows the fringe pattern of the principal stress distribution in a bronze bush. Similar distributions were observed in cases of pairs made of different materials also, with only the magnitude of stress varying. The stress pattern clearly shows that the stresses are distributed symmetrically along the contact length and the maximum stress intensity is observed at both edges of the joint. This localized stress is due to abrupt transition from uncompressed to compressed material at discontinuity in the contact length leads to stress concentration at the contact region as shown in Fig 5.

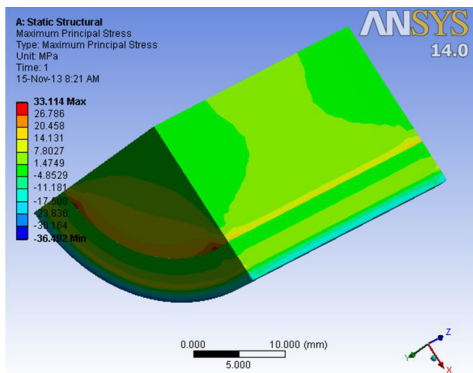


Fig 4: Maximum principal stress in the shaft – bush assembly

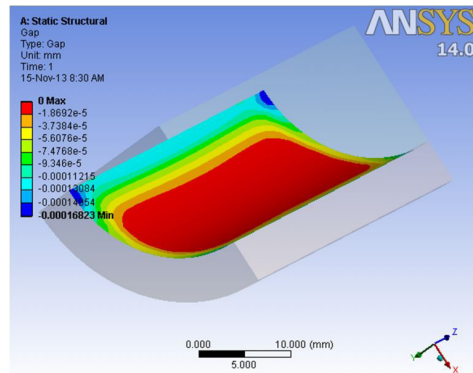


Fig 5: Discontinuity at the contact zone

Contact stress analysis has been performed to examine the contact conditions on the assembly both before loading, and as part of the final solution to verify the transfer of loads (forces and moments) across the various contact regions and the depth of penetration and frictional contact stress were obtained for various combinations of materials of shaft and bush assembly as shown in Fig. 6 and Fig. 7.

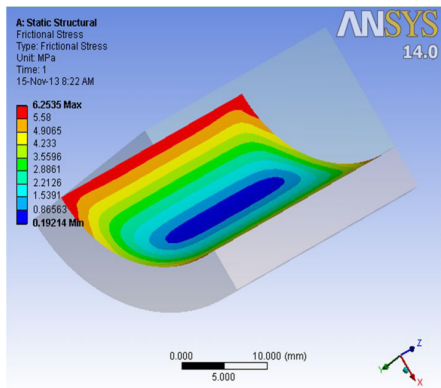


Fig 6: Frictional stress distribution at the contact zone

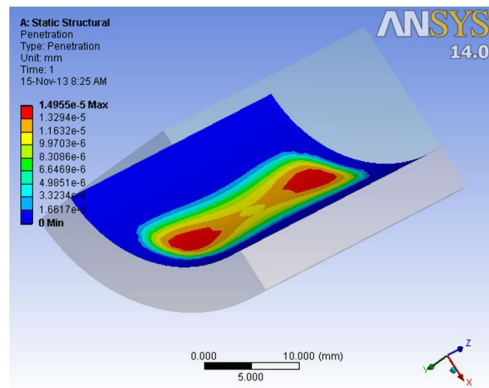


Fig 7: Penetration at the contact zone.

## 5. Comparison of Results

Figure 8 and 9 shows the variation in maximum stress and contact stress in the bush with various material combinations. The stress produced at the mating surface has been taken as the reference value for comparison. The stresses produced from finite element analysis differ slightly from that obtained through Hertzian contact stresses. Stresses produced in case of finite element method are 20% more than the value obtained through hertzian contact stress equations, as the equations are studied only under elastic range. However, there is a deviation from this and practically the mating surface of the shaft contracts (plastically deformed) due to pressure exerted by the inner surface of the bush and the inner surface of the bush expands (plastically deformed) as a result of pressure generated by the bush. This results in strain hardening at the interface of the both shaft and bush.

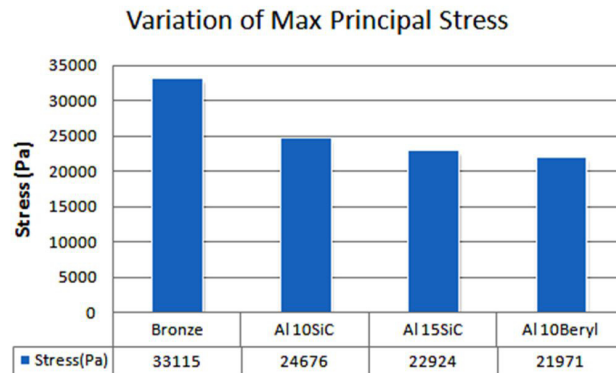


Fig 8: Variation in maximum stress in shaft bush assembly

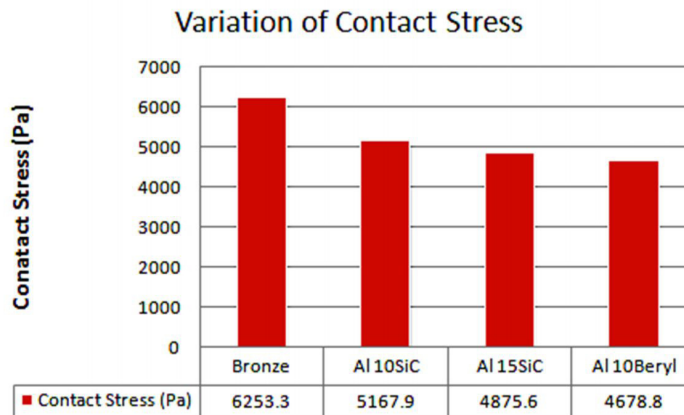


Fig 9: Variation in contact stress in shaft bush assembly

It can be observed that at the interface of the joint, the mating surface of the shaft expands and the inner surface of the bush expands. In other words, both members experience a radial deformation at the joint surface. Hence compressive stresses induce in shaft and bush. Figure 10 shows the variation in the deformation at different speeds for different materials. It can be observed from the Fig. 10, that the deformation in Al-Beryl MMC is less compared to other materials. Also it can be observed that the deformation and stresses does not vary much with change in speed of the shaft.

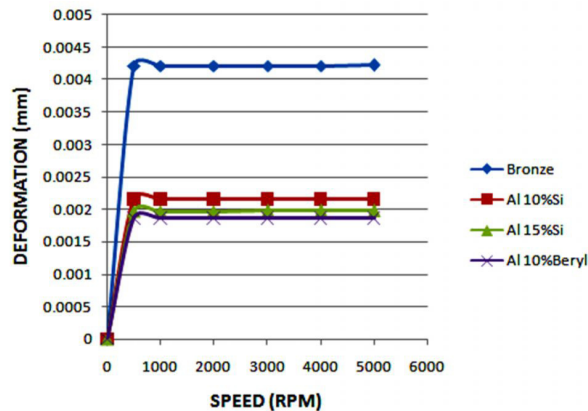


Fig 10: Variation of deformation of Bronze and Al MMCs

## 6. Summary and conclusions

- Contact stresses for the bushes made of Bronze, Al-SiC MMC and Al – Beryl MMC have been systematically evaluated using finite element method. Ansys workbench was used to simulate the analysis.
- Bush made of Al-Beryl MMC showed higher stress withstanding capacity compared to bushes made of bronze bush and Al-SiC MMCs.
- A change in the contact length of the bush does not affect the stress distribution of the contact surface.(i.e., stress concentration is almost same along the contact length)
- It has been observed that there is no significant influence of shaft speed on contact stresses.
- Based on FE analysis, Al-Beryl MMC can be used in for bushes.
- Eventually good agreement was found between finite element method and analytical results based on Hertz's criterion for determination of contact stresses.

## References

- D. D. L. Chung et al. 2003, Composite materials: Functional materials for modern technologies, Springer-Verlag, London
- H. Akbulut et al. 1998, Dry wear and friction properties of  $\delta$ -Al<sub>2</sub>O<sub>3</sub> short fiber reinforced Al-Si (LM 13) alloy metal matrix composites, *Wear*, Vol. 215, No.1-2, pp.170-179.
- H.B. Bhaskar et al. 2012, Tribological Properties of Aluminium 2024 Alloy-Beryl Particulate MMC's, *Bonfring International Journal of Industrial Engineering and Management Science*, Vol. 2, No. 4, pp. 143 - 147
- Irappa Sogalad et al. 2006, A comparative study of stress distribution in interference fitted assemblies, *Indian Journal of Engineering & Materials Sciences* vol 13, pp. 397 – 404
- K. Venkateswarlu et al, 2010, Synthesis of TiN Reinforced Aluminium Metal Matrix Composites through Microwave Sintering, *Journal of Materials Engineering and Performance*, Volume 19(2), pp 231 – 236
- L.A. Dobrzański et al, 2009, Finite Element Method application for modeling of mechanical properties, *Computational Materials Science and Surface Engineering*, volume 1, issue 1, pp 25 – 28
- M.Dhanabalakrishnan et al. 2013, development of particulate reinforced mmc to improve tribological properties for bush bearing, *International Journal of Scientific & Engineering Research* Volume 4, Issue 1, pp. 1 – 8
- M.K. Surappa et al. 2011, Tribological characteristics of A356 Al alloy-SiCP composite discs, *Journal of Wear*, Elsevier, pp. 1946 – 1950
- N.J. Krishnaprasad et al, 2012, Influence of microwave sintering on fabricating Al-Beryl metal matrix composites, *International Journal of Science Research* Volume 01, Issue 04, pp 425 – 429
- Reddappa H.N et al. 2011, Dry sliding friction and wear behavior of Aluminum/Beryl composites, *INTERNATIONAL JOURNAL OF APPLIED ENGINEERING RESEARCH, DINDIGUL*, Volume 2, No 2, pp. 502 – 511
- Vahid Monfared, 2012, Contact Stress Analysis in Rolling Bodies by Finite Element Method (FEM) Statically, *Journal of Mechanical Engineering and Automation*, pp. 12 – 16